Mutations L50F, E166A and L167F in SARS-CoV-2 3CLpro are Selected by a Protease Inhibitor In Vitro and are Associated with Resistance

ICAR 2022
Abstract 214

Cheng Liu[1], Kim Donckers[2], Sarah K Stevens[1], Steven De Jonghe[2], Antitsa Stoycheva[1], Dorothée Bardiot[3], Sandro Boland[3], Lawrence M Blatt[1], Leonid Beigelman[1], Julian A Symons[1], Piet Maes[2], Bert Vanmechelen[2], Pierre Raboisson[5], Patrick Chaltin[3,4], Arnaud Marchand[3], Koen Vandyck[5], Jerome Deval [1], Johan Neyts[2], Dirk Jochmans[2]

[1]Aligos Therapeutics, Inc., South San Francisco, USA. [2]KU Leuven, Department of Microbiology, Immunology and Transplantation, Rega Institute, Leuven, Belgium. [3]Cistim, Leuven, Belgium. [4]KU Leuven, Centre for Drug Design and Discovery (CD3), Leuven, Belgium. [5]Aligos Belgium BV, Leuven, Belgium Presenting Author: cliu@aligos.com

Background

There is an urgent medical need for the treatment and prophylaxis of SARS-CoV-2 infections. The main SARS-CoV-2 protease 3CLpro (Mpro) is a very attractive target which is now clinically validated with the development and emergency use authorization of nirmatrelvir (PF-07321332), a potent 3CLpro inhibitor. As with other direct antiviral agents, the development of viral resistance during treatment is a concern. As a part of our program to develop novel 3CLpro inhibitors, we here report the viral resistance profile of SARS-CoV-2 selected against an early lead compound: Compound 1.

Method

Resistance mutations were selected by passaging SARS-CoV-2-GHB in VeroE6 cells with increasing concentrations of compound 1 in the presence of the P-glycoprotein (Pgp) efflux inhibitor CP-100356. The resistant isolates were analyzed in a VeroE6 CPE assay with multiple 3CLpro inhibitors. Resistance phenotypes were also characterized in a cell-based gain-of-function 3CLpro assay. Recombinant 3CLpro proteins bearing single mutations or multiple mutations were analyzed in a FRET-based enzymatic assay to evaluate the effect of mutations on the activity of 3CLpro inhibitors. Structural biology analysis of the 3CLpro and in silico considerations were used to rationalize the resistance phenotype.

Compound 1 is a potent 3CLpro inhibitor

Compound 1 is a covalent peptidomimetic SARS-CoV-2 3CLpro inhibitor with hydroxyl ketone warhead. The compound inhibits 3CLpro activity in an enzymatic assay, with an IC_{50} value of 14 nM. A VeroE6 cell-based antiviral assay demonstrated that compound 1 efficiently inhibits viral replication with an EC_{50} at 0.59 uM.

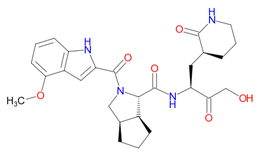

	Compound 1	Nirmatrelvir	PF-00835231
IC_{50} 3CLpro (nM)	14	25	19
IC_{50} Cathepsin L (nM)	>10000	>10000	172
EC_{50} (VeroE6 + CP-100356) (nM)	590	120	190
CC_{50} (VeroE6 + CP-100356) (nM)	>10000	>10000	>10000

Figure 1 – Structure and activity of Compound 1

SARS-CoV-2 acquires phenotypic resistance to 3CLpro inhibitors during passaging with Compound 1

A SARS-CoV-2 isolate, prototypic Wuhan strain, was passaged in VeroE6 cells in the presence of Compound 1. The starting concentration for the selection was 0.4 µM and was increased gradually to 5 µM at p8 (day 28) and 6 µM at p12 (day 39). Amino-acid changes in the 3CLpro were observed at p8 (L50F E166A) and p12 (L50F E166A L167F). Phenotypic analysis of the p12 isolate showed a > 10x increase in the EC_{50}s of Compound 1, PF-07321332 (nirmatrelvir), and PF-00835231 while the sensitivity to remdesivir (GS-441524) remained unchanged.

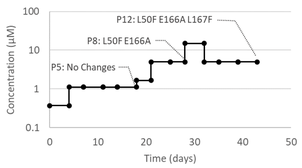

	WT (Wuhan) EC_{50} µM	L50F E166A L167F EC_{50} (µM)	Fold Change
Compound 1 (n=6)	0.59 (0.47-0.83)*	39 (13-47)	63
Nirmatrelvir (n=5)	0.12 (0.094-0.18)	6.1 (5.8 – 8.1)	51
PF-00835231 (n=2)	0.19 (0.18-0.19)	4.4 (1.0 – 7.8)	23
GS-441524 (n=6)	0.79 (0.67 – 1.1)	1.7 (0.59 – 1.9)	2.1

Figure 2 –Left panel: Passaging SARS-CoV-2-GHB in VeroE6 cells in the presence of increasing concentrations of Compound 1. Right panel: Phenotypic resistance associated with the L50F E166A L167F mutation profile. The EC_{50} of different antivirals against SARS-CoV-2 wild-type (WT) or L50F E166A L167F mutant virus was determined on VeroE6 cells (with 0.5 µM CP-100356). *25^{th} – 75^{th} percentile

Cellular 3CLpro assay confirms the mutation-induced resistance phenotype

To further characterize the mutations, a gain-of-function assay for SARS-CoV-2 3CLpro inhibition in living cells, which was developed by Moghadasi et al., was used; and L50F E166A L167F were introduced into the gain-of-function fusion plasmid. The resistance phenotype was confirmed by the increased IC_{50}s for compound 1, nirmatrelvir and PF-00835231 in the cells transfected with mutant 3CLpro plasmid. Nirmatrelvir exhibited the greatest fold change with a value of 28.5.

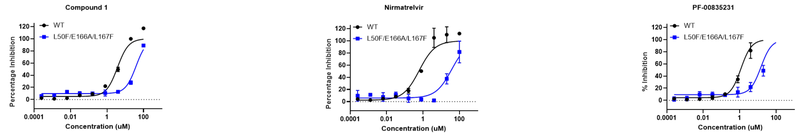

	WT EC_{50} (uM)	Triple Mutant EC_{50} (uM)	Fold Change
Compound 1	2.18	29.45	13.5
Nirmatrelvir	0.93	26.50	28.5
PF-00835231	3.19	11.05	3.5

Figure 3 – Upper panel: inhibition curves of Compound 1, nirmatrelvir and PF-00835231 against WT, L50F/E166A/L167F triple mutant in cellular protease assay. Lower panel: IC50 values and fold changes of the three compounds against WT and the triple mutant.

Mutations significantly impact the enzymatic activity of recombinant 3CLpro

Each mutation, alone and in combination, was introduced into recombinant purified 3CLpro enzymes. All the mutations significantly decrease the enzymatic activity of 3CLpro. The single mutant, L50F, showed the lowest activity with only 0.5% of WT 3CLpro. All other mutants (E166A and L167F single mutants, L50F E166A L167F) vary from 5% to 16% activity of the WT protein.

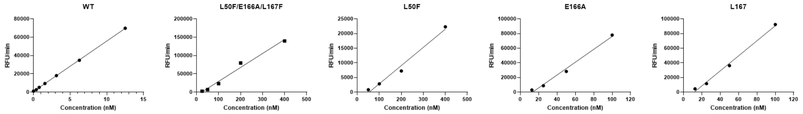

	Velocity at 100 nM (RFU/Min)	Percentage activity of WT
WT	551511	100.0
L50F E166A L167F	29455	5.3
L50F	2858	0.5
E166A	76082	13.8
L167F	90690	16.4

Figure 4 – Upper panel: Enzyme titration of wild type, triple mutant L50F/E166A/L167F, single mutant L50F, E166A and L67. Lower panel: Initial velocity at 100 nM of WT and mutant enzymes were calculated using titration curves, and the activity was converted into percentage of WT 3CLpro

Single mutations (E166A and L167F) and triple mutation (L50F E166A L167F) confer resistance to 3CLpro inhibitors

While two of the single mutations (E166A and L167F) provided low-level resistance to the inhibitors in a biochemical enzymatic assay, the triple mutant displayed the highest levels of resistance, ranging from 11- to 80-fold, which is consistent with the results from antiviral assay and cellular 3CLpro protease assay.

	IC_{50} (nM)	Fold Change		
	Wild Type*	L50F E166A L167F	E166A	L167F
Compound 1	14	35	6	5
Nirmatrelvir	25	80	17	5
PF-00835231	19	11	2	4

Figure 5 – IC_{50} Fold changes of Compound 1, nirmatrelvir and PF-00835231 against WT, L50F/E166A/L167F triple mutant, E166A and L167F single mutants. *Enzymatic assays were run at a 50 nM concentration of enzymes including WT 3CLpro.

Resistance mutations decrease the dimerization affinity of the 3CLpro dimer

A unique pattern was observed in the dose response assay for 3CLpro mutants against inhibitors. The activity increased at low inhibitor concentrations, and was inhibited at high inhibitor concentrations, which is reminiscent of the MERS 3CLpro. The dimerization of MERS 3CLpro has low affinity and can be induced by inhibitors, hence its activity is enhanced by low inhibitor concentrations. The dissociation constants of dimerization of mutants were calculated accordingly. The K_d values of mutants are much higher than WT, which suggests mutations decrease the dimerization affinity. E166 was reported to be involved in dimerization of SARS-CoV-1 3CLpro (Cheng et.al. 2010)

A

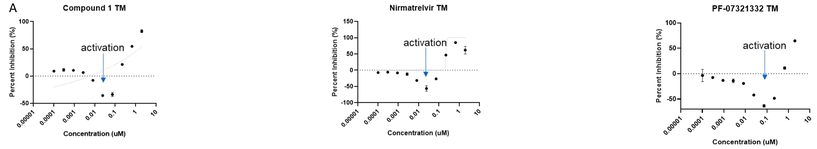

B

Protein	Dimerization K_d (nM)
WT	<1.5
L50F E166A L167F	966
L50F	2287
E166A	235
L167F	127

C

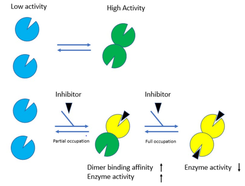

Figure 6 – **A**: Inhibition curves of PF-00835231, nirmatrelvir and Compound 1 against WT, L50F/E166A/L167F triple mutant, TM: triple mutant. Curves utilizing the triple mutant clearly show the activation of enzyme at low inhibitor concentration. **B**: Dimerization Dissociation Constant (Kd) for WT and mutants. **C**: Proposed mechanism for inhibitor activation.

In Silico analysis of Compound 1 interactions with WT 3CLpro rationalizes the resistant phenotype

Compound 1 binds covalently to the catalytic C145 and forms seven Hydrogen bonds with 3CLpro: warhead to C145 in the oxyanion hole; P1 lactam to H163, E166 and F140; peptide backbone to H164 and E166; P3 indole to E166. The fused bicyclic P2 substitution maximizes Van der Waals interactions in the S2 sub-pocket. E166A results in ~33% loss of Hydrogen-bonding capacity to the S1 sub-pocket. L167F flanks the Compound 1 indole in the S3 sub-pocket. The L50F side chain is located within 2.7 Å of Q189 which may disrupt Q189 Hydrogen-bonding to the Compound 1 backbone via ordered water molecules.

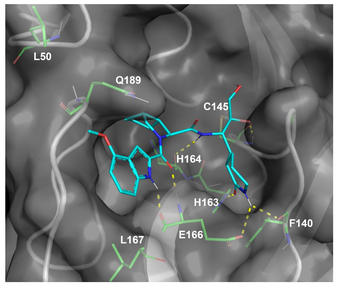

Figure 7 – Compound 1 (Carbon: cyan, Nitrogen: navy; Oxygen: red) covalently docked to WT 3CLpro (gray cartoon and surface; key side chains shown with Carbon: green, Nitrogen: navy; Oxygen: red).

Conclusion

We report here the first SARS-CoV-2 resistance selection in vitro with 3CLpro inhibitors. The acquired mutations (L50F, E166A, L167F) confer resistance to multiple 3CLpro inhibitors in cellular antiviral assays, gain-of-function cellular protease assays, and biochemical enzymatic assays. The mutations also decrease the enzymatic activity and dimerization affinity of 3CLpro. Our results provide additional information on the potential role of the E166A substitution as proposed previously (Flynn et al, 2022). The clinical significance of these mutations remains to be determined and the effect on viral replication capacity is being evaluated.